HUNGARIAN UNIVERSITY OF AGRICULTURE AND LIFE SCIENCES

Analysis of Irrigation Efficiency Based on Remote Sensing

Test Area: New Halfa Scheme, Sudan

Thesis of the PhD dissertation

Taha Ibrahim Mohammed Ahmed Ibrahim

GÖDÖLLŐ, HUNGARY

2023

The PhD School

Name: Doctoral School of Environmental Sciences

Discipline: Water Resources Management

Head: Professor Csákiné Dr Erika Michéli, Institute of Environmental Sciences, Hungarian University of Agriculture and Life Sciences.

Supervisor (s):

Dr Zoltán Vekerdy, Professor, Department of Water Management and Climate Adaptation, Institute of Environmental Sciences, Hungarian University of Agriculture and Life Sciences.

Dr István Waltner, Associate Professor, Department of Water Management and Climate Adaptation, Institute of Environmental Sciences, Hungarian University of Agriculture and Life Sciences.

Csákiné Michéli Erika ....

Approval of Head of Doctoral School

....

Approval of Supervisor/s

1. INTRODUCTION

1.1 Background

Water management for agricultural purposes is a complex task because it depends on several factors: social, environmental, and political factors such as population growth rate, change in water use patterns, climate changes, change in hydraulic systems of rivers and the development of water resources in riparian countries. Its performance can be far below its potential, especially in drought-prone areas, making agricultural production and irrigation economically inefficient (K. Raju, 1999). Effective irrigation systems are inevitable in providing adequate food to the world. Agriculture consumes about 60 to 70 % of the world's freshwater resources in the irrigation process, and the irrigation systems have efficiency ranging from 30 to 60 %. Although the available resources are mostly renewable, they have a limit for regeneration that cannot be exceeded (Darshana, Pandey, Ostrowski, & Pandey, 2012).

Monitoring soil and crops during the growing season is essential for agricultural production. Plant characteristics change according to the plant's phenological stage from the seedling until it reaches full maturity. As a function of this process, there is also a dynamic of the optimal crop transpiration, i.e., the crop water requirements. In the primary stages of growth, most of the evaporation occurs from the soil's surface. However, as plants grow, the contribution of transpiration as one of the components of evapotranspiration increases until maturity and gradually decreases afterwards. The collection of information about crop evapotranspiration is very important in the irrigation scheduling process to raise the efficiency of water use (Allen, Pereira, Raes, Smith, & Ab, 1998).

Methods for assessing the performance of irrigation using data from satellites have been developed since the second half of the 1980s. There is a consensus that it is difficult to gather reliable and continuous terrestrial information on it. Initially, the focus was on the relationship between quantifying water use and cultivated area, but later attention was given to other aspects such as the crop water requirements, water productivity, water stress and salinity of water (Akdim et al., 2014).

Irrigation performance indicators were first introduced in the 1970s and described the hydraulic behaviour of irrigation systems (Bastiaanssen et al., 2001). Later, crop-oriented indicators were also developed. For example, the overall consumed ratio quantifies the degree to which crop irrigation requirements are met by irrigation water in the irrigated area (Bos & Nugteren, 1990).

Crop water deficit over a period is defined as the difference between ET_p and ET_a of the cropping pattern within an area (Bastiaanssen et al., 2001).

Remote sensing images captured by sensors on satellites or airplanes can be considered, among others, as tools to give spatial information about evapotranspiration. However, the lack of availability of these images with sufficiently high temporal resolution and accuracy is one of the obstacles to using this technique. However, with the evolution of communication and computing technology, together with the policy changes of the national aeronautics administrations, like the NASA of the United States of America's government (i.e., they provided free access to satellite data), an increase was observed in the development of this technology (Calera, Campos, Osann, D'Urso, & Menenti, 2017).

In the past decade, many models have been developed that simulate plant growth and water balance. These models help us understand the process of plant development and are solutions to control the use and distribution of water (Wang, Zhang, Dawes, & Liu, 2001). Evapotranspiration is the main component of the water balance that consumes the largest amount of irrigation water and rainfall in cultivated areas. Several models have been developed for the quantification of actual ET, which are based on the surface energy balance, such as the Surface Energy Balance System (SEBS) (Su, 2002), the Simplified Surface Energy Balance Index (S-SEBI) (Roerink, Su, & Menenti, 2000), the Operational Simplified Surface Energy Balance (SSEBop) (Senay et al., 2013), satellite-based energy balance for Mapping Evapotranspiration with Internalized Calibration (METRIC) (Allen, Tasumi, & Trezza, 2007), the Surface Energy Balance Algorithm for Land (SEBAL) (Bastiaanssen *et al.*, 1998).

Estimating evapotranspiration (ET) on a field scale has been accomplished using high spatial resolution but low temporal resolution satellite data from the Landsat TM and ASTER. However, due to the long repeat cycle of these satellites, these data sets are unsuitable for routine ET estimation. Others have attempted to use daily or more frequent satellite data from the AVHRR and GOES, which have coarser pixel resolutions of 1 to 5 km, resulting in ET estimates that represent averages over areas of 1 to 25 km2. Unfortunately, this method cannot distinguish the ET of individual fields. The MODIS proposed pixel resolutions ranging from 250 m to 4 km have been used to assess land cover changes accurately, showing that a pixel resolution of 500 m or less is necessary. Even at the 1-km pixel resolution, detecting the areal extent of such changes is often unreliable. Land Surface Temperature LST can monitor significant changes in surface energy balance and ET with land use and land cover changes.

However, higher temporal frequency-coarser resolution thermal-infrared data is required to monitor such changes routinely, which should be at the 250- to 500-m pixel size (Kustas, Norman, Anderson, & French, 2003).

It is known that water shortage leads to the reduction of crop productivity, and the purpose of irrigation is to reduce plant stress. There are several factors to consider in planning irrigation, such as crop water requirement, costs, water availability and other factors, especially in the arid zones. The response of crop yield to irrigation has been studied extensively. Through proper irrigation management, it should be possible to provide only the water that matches the crop ET (Wang et al., 2001).

1.2 Objectives

1.2.1 Main objective

Develop a remote sensing-based method that supports improving water use efficiency for irrigation.

1.2.2 Specific objectives

To achieve the main objective, the following specific objectives are set:

1. Improve the DisTrad method of downscaling LST for large areas with complex land cover.
2. Create high spatial and temporal resolution time series of actual evapotranspiration maps using remote sensing to define the spatial distribution of the actual ET.
3. Propose an optimal integration method of the optical data to overcome the cloud cover problem.
4. Analyse the irrigation efficiency for the New Halfa irrigation scheme:
    a. Evaluate the irrigation performance in the New Halfa scheme to define the spatial and temporal distribution of the water applied and demanded.
    b. Analyse the current irrigation schedule of wheat in the New Halfa scheme to identify the spatial distribution of the water stress.
    c. Estimate the crop water productivity for wheat crop.
5. Propose a method to optimize the irrigation schedule for wheat.

2. RESEARCH METHOD

2.1 Study area

The construction of the Aswan High Dam caused the inundation of the old town of Wadi Halfa by Lake Nasser. The New Halfa Agricultural Scheme was initiated in response as Sudan's largest resettlement project at the time. The New Halfa Agricultural Scheme is a 185,000 ha agricultural settlement scheme on the western side of Kassala State, roughly 400 km east of Khartoum (Laxén, 2007). The project is located on the Butana Plain, along the Atbara River. At the time of its construction, the New Halfa Scheme was Sudan's second-largest irrigation project after the Gezira Scheme, which is still the world's largest irrigation scheme. Sudan's irrigation agency manages the water through the Khasm el Girba dam on the Atbara River (Wallin, 2014). Climatology: the area lies in the dry climatic zone, with annual rainfall varying from 200- 300 mm, concentrated mainly in July and August. The highest mean daily maximum temperature is 42°C in May, and the lowest mean daily minimum temperature is 14°C in January. Humidity is low most of the year, and solar radiation is very high (Adam, 2002). The irrigation system is gravity-fed, with the main canal transporting water to the project area via a network of subsidiary canals and motorized pumps in the small scheme areas. The irrigation system includes main canals, branch canals, minor canals, quaternary canals, and tertiary farm ditches. Field irrigation is done using the traditional flooding (Angaya) approach. There are significant water losses in the system, reducing the available freshwater supplies, like evaporation, conveyance losses due to infiltration, etc. (Wallin, 2014). The dam was initially intended to store 1.3 billion cubic meters of water. However, by 1976, the reservoir's storage capacity decreased to 0.8 billion cubic meters due to significant siltation originating from the upstream catchment of the river Atbara in Ethiopia's highlands (Laxén, 2007). The reservoir's capacity is now about 0.6 billion m^3. During the growing season, water in the smaller canals typically flows permanently. Farmers, however, have complained that some regions receive less water than others. Since the reservoir's capacity is dwindling, the irrigated area is shrinking too. Each agricultural settler was given a 15-feddan hawasha (6.3 ha tenancy) to cultivate cotton, wheat, or sorghum, as well as groundnuts. Cotton was mostly chosen since it was the most important cash crop for the government to provide hard currency and profit for the tenants. Groundnuts are the scheme's second most significant cash crop, and wheat and sorghum were grown as food security crops (Wallin, 2014).

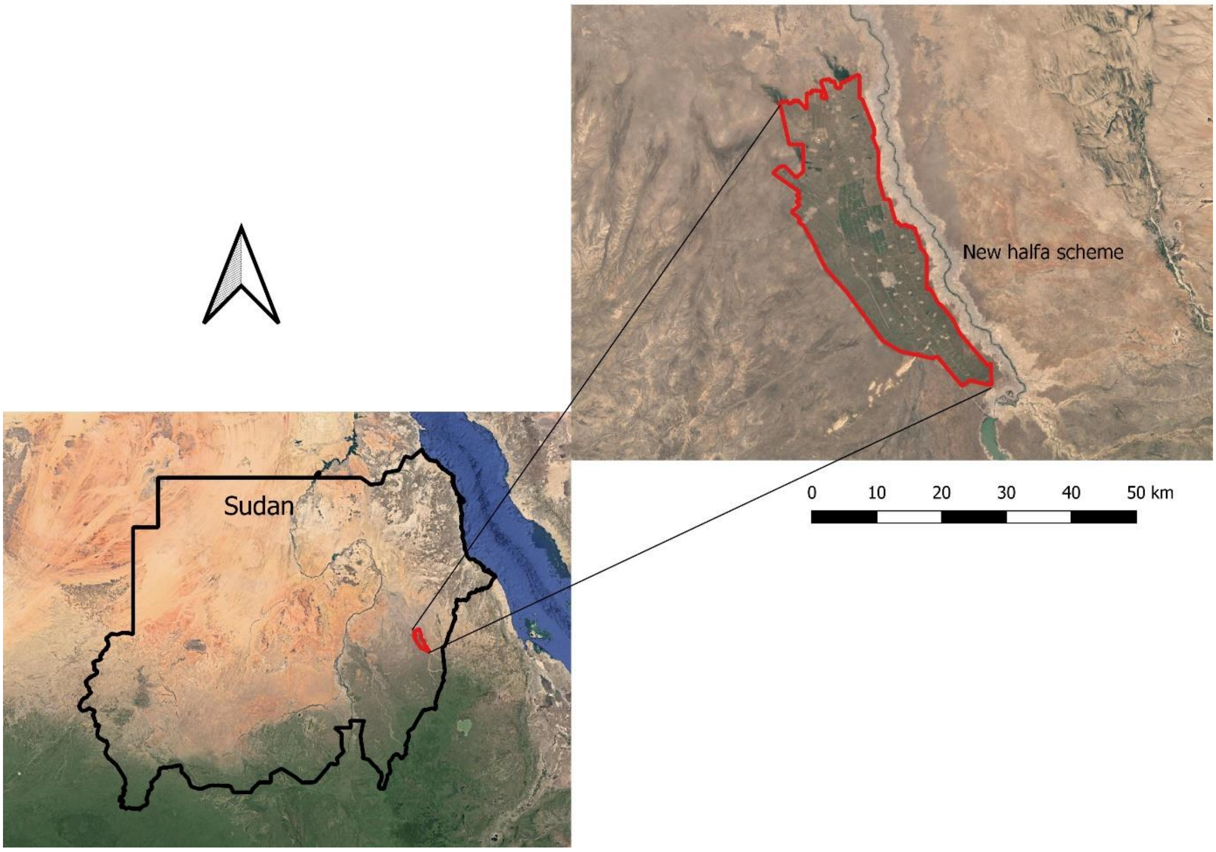

Figure 1. Location map of the study area.

2.2 The framework of the research

This study comprises crop water productivity calculation, irrigation performance assessment and scheduling irrigation for the wheat crop in the New Halfa project. It is based on several types of data and analyses, such as evapotranspiration, water balance of soil, water requirement for wheat crop and methods of irrigation performance assessment, as shown in Figure 2.

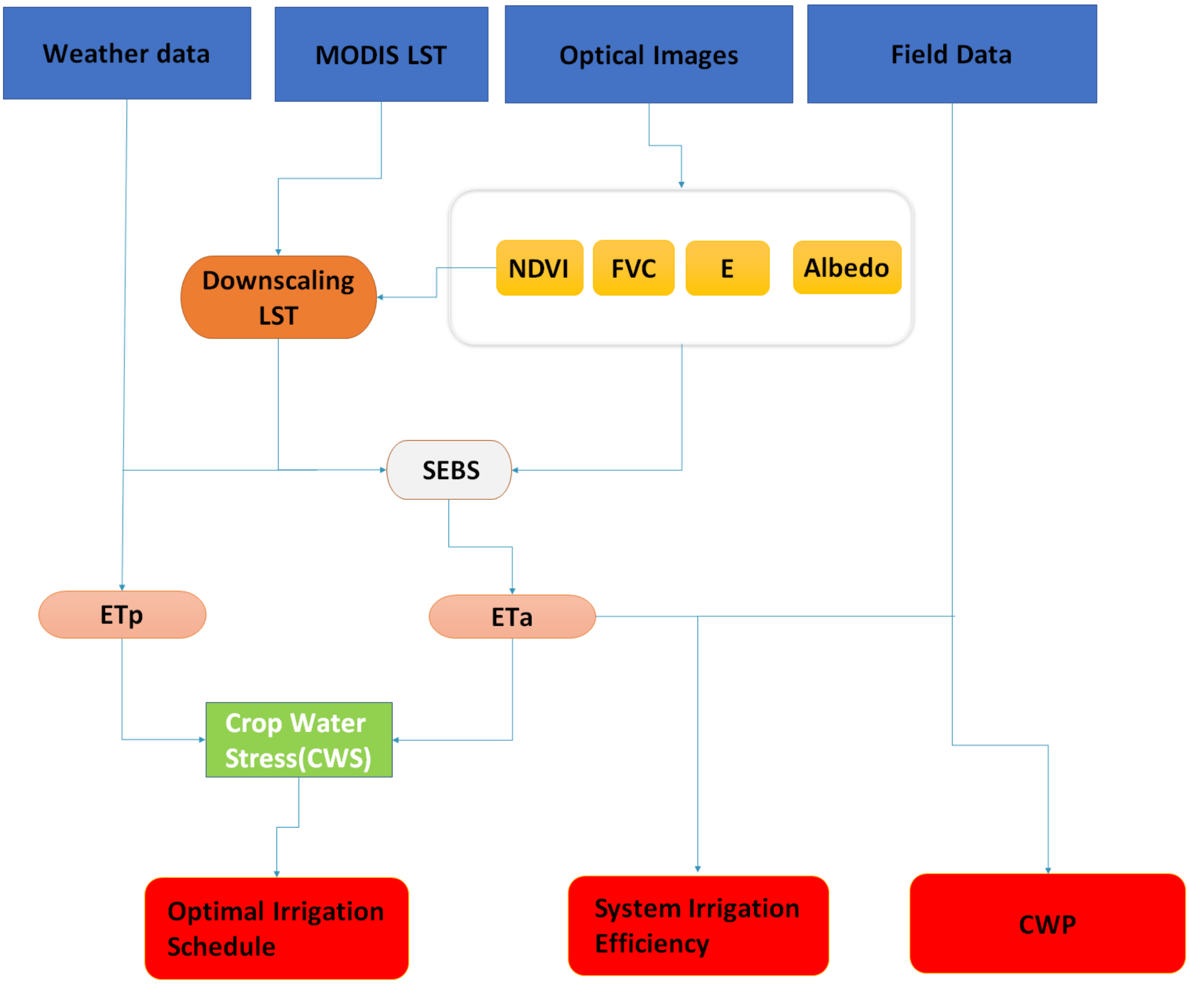

Figure 2. Flow chart of the research

2.3 Land surface temperature downscaling

2.3.1 The DisTrad downscaling procedure for radiometric surface temperature

To find a mathematical relationship between the radiometric surface temperature and the normalized difference vegetation index, Kustas et al. (Kustas et al., 2003) suggested aggregating the fine-resolution NDVI map to the same coarse-resolution as of the LST map and then to defining regression coefficients of Equation (1) with a least square fitting using a second order polynomial.

$$LST^*_{CR} = a + b\ NDVI_{CR} + c\ NDVI^2_{CR} \quad (1)$$

Where LST^*_{CR} is the land surface temperature at the coarser resolution (°C) and $NDVI_{CR}$ is the aggregated normalized difference vegetation index at the coarser resolution (-).

In practice, for defining the NDVI-LST relationship, the coarse-resolution NDVI map was divided into three NDVI classes and the coefficient of variation of the fine-resolution NDVI values within each coarse-resolution pixel was calculated. To avoid the influence of heterogeneity, this map was divided into three classes: NDVI < 0.2 for the bare soil, 0.2 < NDVI < 0.5 for the partial vegetation, and NDVI > 0.5 for the full vegetation. Finally, 25% of the pixels with the lowest coefficient of variation were selected from each group to obtain the correlation (Kustas et al., 2003).

2.3.2 DisTrad modification

The study area may be classified as a mixed landscape with various distinct land cover types (dense vegetation, medium-dense vegetation, low-density vegetation, bare soil, urban areas, and water). The DisTrad approach is based on the correlation between the LST and NDVI. The original approach uses a second-order polynomial regression, assuming a non-linear relationship between the two variables. However, in certain cases, outliers at the edges of the value range may strongly affect the second-order polynomial. To circumvent this issue, we tested whether a linear regression would improve the robustness of the regression equation.

Furthermore, the original DisTrad technique recommends using 25% of the aggregated pixels with the lowest coefficients of variation for parameterising the regression equation. Nonetheless, in the case of a heterogonous area (e.g., due to small agricultural fields relative to the coarse pixel size), where the CV of the original NDVI values within most of the coarse-resolution pixels is relatively high, we tested the effect of using only 10% of the aggregated pixels with the lowest coefficients of variation in defining the parameters of the regression equation.

2.4 Evapotranspiration estimation

Evapotranspiration (ETa) is a significant water loss process in arid and semi-arid regions. Measuring ETa through earth observation requires high spatial resolution input data, which is unavailable for Land Surface Temperature (LST). This necessitates downscaling low-resolution data like MODIS. A dataset of 67 MODIS and 7 Landsat images from December to March 2017/2018 was collected, registered, and projected. The Surface Energy Balance System (SEBS) model, using Landsat-8 and Sentinel-2 remote sensing data, was employed to map wheat ETa. Meteorological data like wind speed and air temperature were sourced from the Meteorological Bureau of New Halfa. SEBS combines remote sensing and meteorological data to calculate net radiation, soil heat flux, and sensible heat flux. Applying the energy balance equation, instantaneous ET is computed during satellite passes. Daily ETa is derived assuming a constant evaporation fraction. When satellite images are unavailable, the Penman-Monteith method is used for ET calculation. Calculation details are available in Su (2002).

2.6 Irrigation performance

In this study, two irrigation performance indicators were used to assess the irrigation performance in the New Halfa scheme.

2.6.1 Classical irrigation efficiency

This concept was used to assess the irrigation system performance, as shown in Equation (2).

$$E_i = \frac{ET_i}{W_g - P_e} \quad (2)$$

Where ET_i is the water that was used by E and T, W_g is the gross supply which represents the water delivered by the canals, and P_e is the effective precipitation or precipitation that decreases the quantity of irrigation water required. Since the value of the effective precipitation during the winter season is approximately zero, that means the equation will be as Equation (3).

$$E_i = \frac{ET_i}{W_g} \quad (3)$$

3.6.2 Water productivity

Water productivity has been proposed as a metric for analysing water consumption and evaluating irrigation efficacy. WP (grain yield per unit of actual ET) was calculated in this study using Molden's indicator (Molden, 1997), Equation (4).

$$\mathrm{WP} = \frac{Y}{ET_{cs}} \quad (4)$$

Where WP is water productivity, Y is the wheat seasonal crop yield in $kg\ ha^{-1}$ and ET_{cs} is actual seasonal evapotranspiration for wheat crop in $m^3\ ha^{-1}$.

2.7 Scheduling irrigation for wheat crop

2.7.1 Crop water stress

For scheduling irrigation, the crop water stress index has been used as an indicator for the crop water status, which has a key role in applying the irrigation events. The evapotranspiration has been used to estimate the Crop Water Stress Index (CWSI), where we can define the CWSI as the ratio between actual and potential evapotranspiration. A crop with adequate water supply will transpire at the same rate as the potential evapotranspiration. When the water becomes limited, the actual evapotranspiration will fall below the potential evapotranspiration. This ratio ranges from 0 to 1, where 0 means no stress, and 1 is a high rate of water stress.

Several writers have hypothesized that stomatal closure is caused by a lack of soil water and a high evaporative demand. This is based on the idea that high evaporative demand necessitates a high rate of water intake and transport, resulting in a larger energy loss between the water in the soil and the stomates. Because evaporative demand varies diurnally and from day to day, methods for estimating evapotranspiration on a daily basis with high accuracy are required.

The SEBS model was used to calculate the daily actual evapotranspiration. The potential evapotranspiration was calculated by multiplying ET_0 and the crop coefficient k_c

$$ET_c = k_c \times ET_0 \tag{5}$$

Finally, the CWSI can be calculated as equation (6).

$$\text{CWSI} = 1 - \frac{ET_a}{ET_c} \tag{6}$$

The CWSI of the wheat crop for the growing season 2017-2018 was calculated in three different sites of the scheme for all the available days.

3. RESULTS AND DISCUSSION

3.1.1 Relationship between land surface temperature and the vegetation cover

The DisTrad method recommended the use of 25% of the aggregated pixels with the lowest coefficient of variation for defining the regression equation. However, for heterogeneous areas like small fields, this can yield a low coefficient of determination due to mixed pixels. To address this, 10% of the lowest coefficient of variation pixels were used for correlation. To test this approach, NDVI-LST correlation was analysed at 1 km resolution with 10% and 25% of the data. Results indicate a higher correlation (R2) using 10% (0.80) compared to 25% (0.75) of the lowest coefficient of variation data, as shown in (Figure 3).

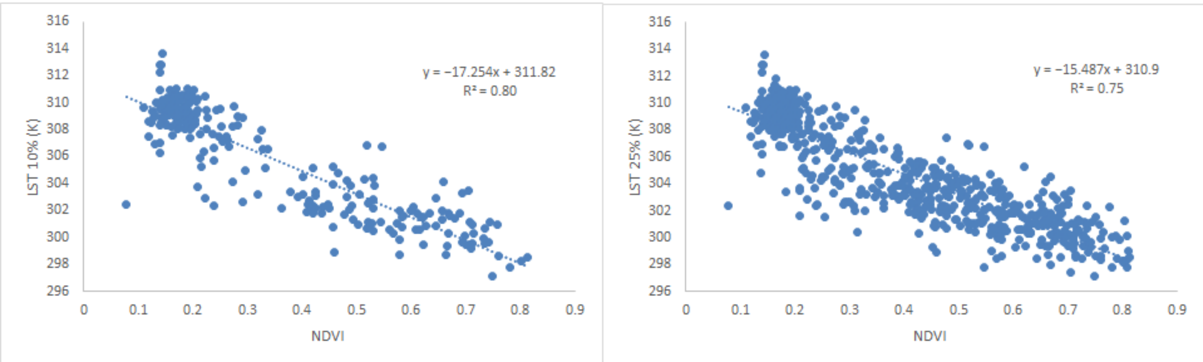

(a) (b)

Figure 3. (a), (b) correlation between the NDVI and LST for 25% and 10% methods, respectively.

2.1.2 Effects of LST downscaling on the Landsat 8 image

Figure 4. shows the correlation between the LST_{native} (x axis) and LST 10% and LST 25% (y axis) of the linear regression. The coefficient of determination (R^2) is 0.72 and 0.74, respectively, while it was 0.61 for the polynomial regression. This result indicates that using linear regression for the downscaling process gives better results than the polynomial regression since the polynomial regression with 25% of the pixels results in several extreme values. The same result was observed by Agam, Kustas, Anderson, Li, & Neale (2007). This is due to the increasing degree of subpixel variability. Based on this statistical analysis, the proposed modification yields superior results.

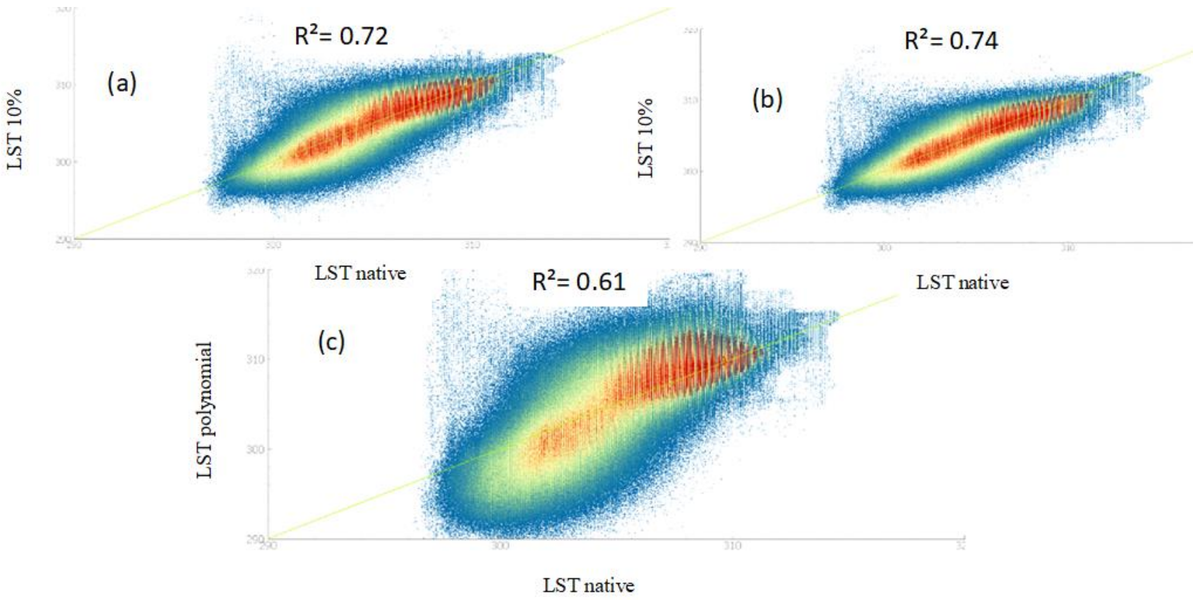

Figure 4. (a), (b), (c) scatter plots between native LST compared to LST10% (linear), LST 25% (linear) and LST 25% (polynomial), respectively

3.1.3 Effects of LST downscaling on ETa estimation

The Surface Energy Balance System utilized the downscaled land surface temperature to estimate the actual evapotranspiration with high spatial resolution, as described in (section 3.4).

Concerning the effect of downscaling the land surface temperature on the evapotranspiration estimation, we found that the downscaling using only 10% of the pixels results in a good correlation between the ETa calculated from the LSTnative and ETa calculated from LST10% and LST25%, due to the high degree of convergence between the results from these two methods and the native Land Surface Temperature. The coefficients of determination for the linear regression with 10% and 25% of the pixels were 84.5 and 84.1, respectively (Figure 15). This yielded a RMSE of 0.3 and 0.28 mm/day, respectively. The evapotranspiration maps produced using downscaled land surface temperature had a higher spatial resolution than those produced using native land surface temperature, as the details and boundaries of small fields are more accurate on these maps than on the maps produced using native land surface temperature, as shown in Figures 5. Bindhu, Narasimhan and Sudheer (2013) got RMSE in the similar range of 0.16 with TsHARP = 0.55 mm/day using the non-linear disaggregation approach (NL-DisTrad).

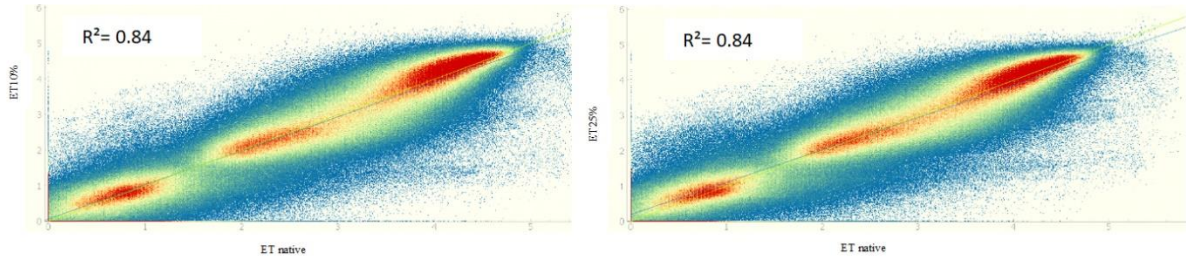

Figure 1. (a) and (b) scatter plots for the correlation between ETa (LST native) and ETa (LST10%), (LST25%), respectively.

3.2 A combination of different optical data for downscaling

The poor temporal resolution of the Landsat 8 images limits their use in estimating daily evapotranspiration for water management. This poor temporal resolution prevents the use of the Normalized Difference Vegetation Index produced by Landsat 8 for the daily LST downscaling process. Cloud distortion can be another limiting factor that affects the Landsat images' usability for evapotranspiration estimation.

To fill the gap left by the Landsat images, images of Sentinel-2 with a higher spatial and temporal resolution were used (spatial resolution is 10-20 m, and the temporal resolution is at least 5 days). In this study, 6 images from Sentinel-2 were processed. We tested the correlation between the NDVI generated by the two sensors, as shown in Figures 18 and 19. The goal of this test was to check whether the Landsat 8 and Sentinel-2 images could be integrated into a consistent time series of NDVI maps with 30 m field resolution for the LST downscaling procedure.

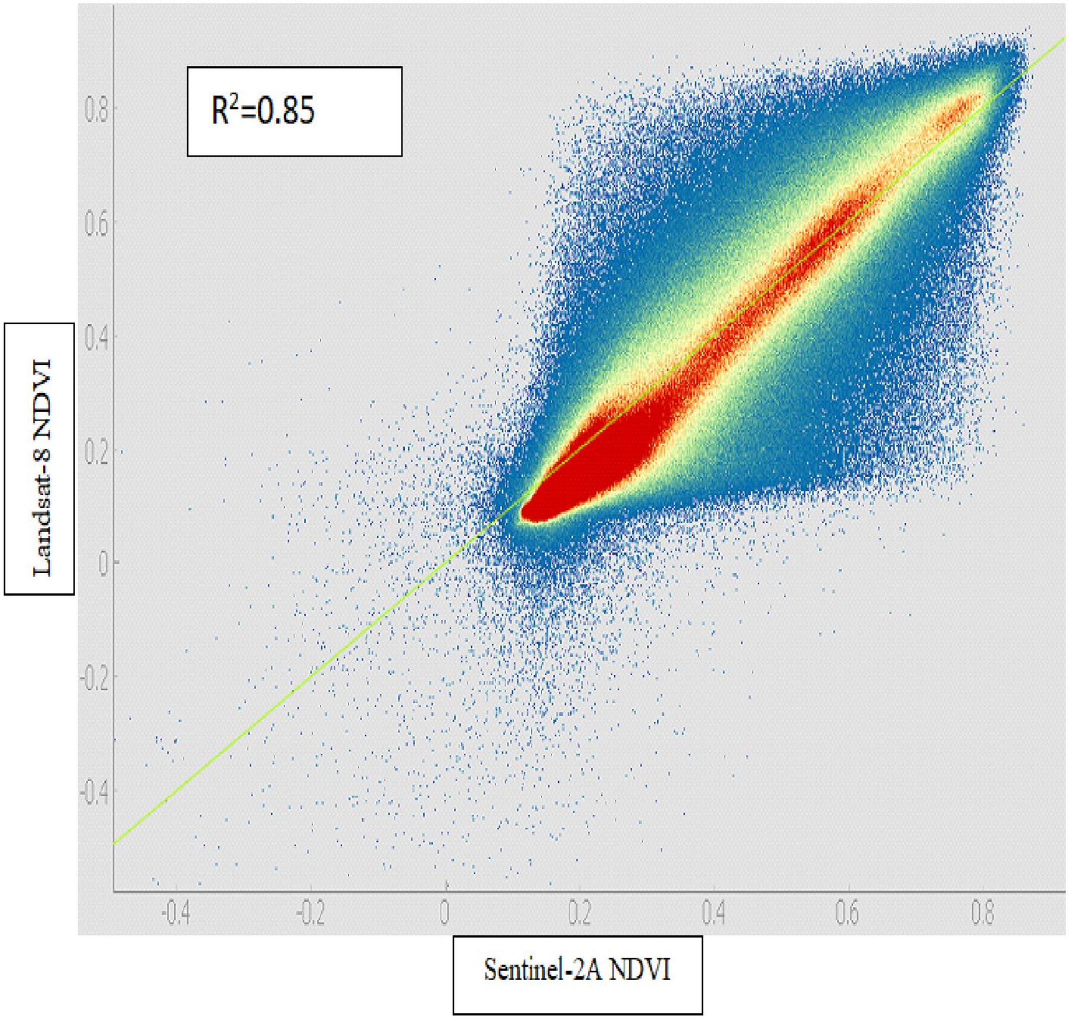

Figure 2. Scatter plot for the correlation between Landsat-8 (17.12.2018) NDVI and Sentinel-2A (21.12.2018).

3.3 Evapotranspiration time series estimation and validation

Fifty-five downscaled land surface temperature maps were used to estimate the actual evapotranspiration of the wheat crops from December 2, 2017, to March 9, 2018. Eight pixels from eight fields were chosen, and the mean calculated for these pixels was compared to potential evapotranspiration. Figure 7 shows the daily evapotranspiration (mm day^{-1}) calculated using SEBS, ranging from 1.5 mm d^{-1} at the start of the season to 5.8 mm d^{-1} in the mid-season and 1.3 mm day^{-1} at the end of the season.

The result was compared to the potential evapotranspiration ET_p estimated from the reference evapotranspiration based on meteorological parameters and the crop coefficient, as illustrated in Figure 7. However, as shown in Figure 7, there was a strong correlation between the two products, with R^2 = 76. Figure 7, on the other hand, depicts realistic trends in the accuracy of ET_a generated from SEBS. Figure 7.

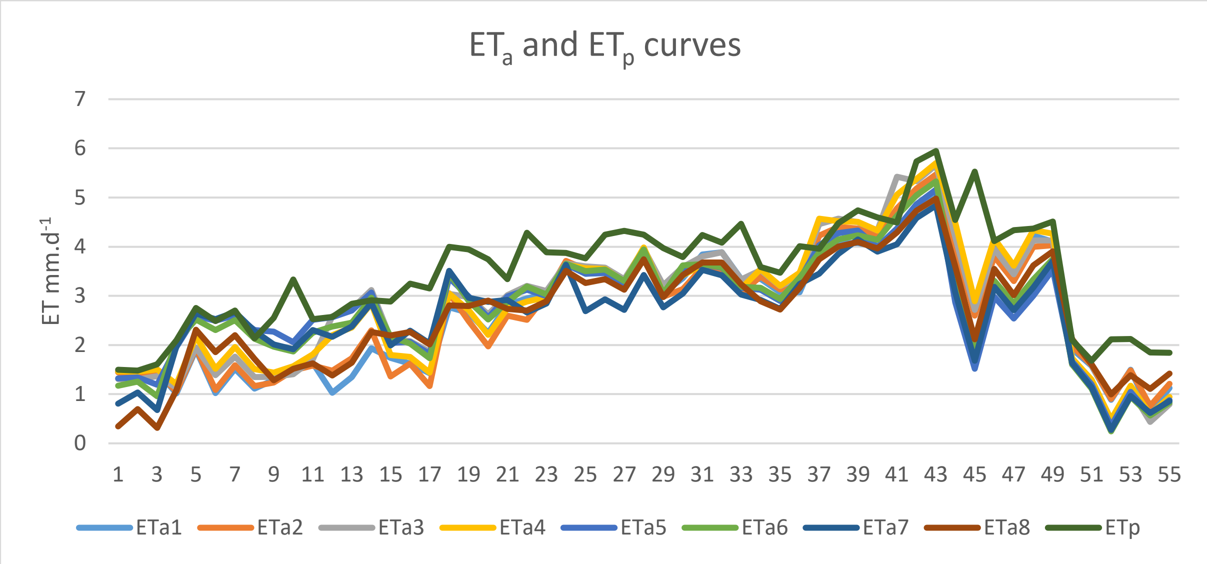

Figure 3. ETa and ETp curves for the winter season 2017-2018 ARC site.

During the wheat growing season, the study shows continuously changing patterns in ETa. ETa gradually increases from the beginning of the season, peaking in the middle, and then decreases as the season progresses until crop maturity. The seasonal ETa for wheat in the New Halfa scheme was calculated by integrating daily ETa images from December 1st to March 9th, amounting to around 350 mm.

Limitations of point measurement methods for regional ETa calculations are highlighted, including their inability to account for dynamic vegetation changes, crop density, and crop stress due to water scarcity. The absence of field data in the New Halfa Scheme prevented qualitative validation of the results. However, a quantitative analysis was performed by comparing SEBS-calculated ETa with ETp (potential evapotranspiration) obtained from meteorological data. Figure 7 shows good agreement between SEBS and measured ETp patterns, even considering the influence of water stress. Additionally, the study's results were compared with those of other researchers in similar areas, showing agreement between the findings.

4.6 Water application efficiency

Water Application Efficiency (WAE) is a metric that quantifies the effectiveness of irrigation by measuring the ratio of delivered water to the farm compared to the water actually utilized through transpiration, evaporation, or a combination of both within the soil's root zone. In the context of the study, WAE was calculated using SEBS-estimated ETa (evapotranspiration) data that was converted to volume. The water delivered to canals was measured in the field, marking the first attempt to spatially analyze water application efficiency in Sudan's New Halfa Scheme. The study period was from December 2nd to February 11th, 2018, with calculations made every ten days to represent the interval between irrigation events, which were scheduled according to Table 1.

Table 1. Water application efficiency (WAE) 01.12.2017- 11-02-2018.

Irrigation events	ETa volume m^3	Water delivered m^3	WAE
10-12-2017	37548.8	63850	59%
20-12-2017	36962.12	63900	58%
30-12-2017	24713.86	61975	40%
10-01-2018	40631.37	66675	60%
20-01-2018	31610.862	51400	61%
31-01-2018	54217.62	68505	79%
11-02-2018	36483.72	59800	61%

Table 1 presents the average values of WAE. Notably, the study found that the calculated WAE was significantly lower than the recommended surface irrigation standard of 75%. Several factors were identified as contributing to this low WAE:

Parasitic Weeds: The prevalence of parasitic weeds in the irrigation system of the New Halfa Scheme negatively impacted water distribution within the branch channels and fields.

Uncontrolled Silting Removal: The removal of sediment (silting) in the channels was carried out in an unregulated manner. This led to increased channel depths, hindering efficient water distribution. The gravity-driven flow of water in these channels resulted in surface runoff at the scheme's end.

Inadequate Water Management: The water management approach in the scheme relied on estimating evapotranspiration from a single point measurement, which was then used to represent the entire project. Additionally, irrigation operations followed a fixed schedule without considering plant conditions or prevailing climatic factors.

In summary, the study revealed that the New Halfa Scheme's WAE was much lower than the desired standard due to issues such as parasitic weeds affecting water flow, uncontrolled silting removal altering channel depths, and an inadequate water management strategy that disregarded plant status and climate variations.

4.8 Crop water stress

In arid and semi-arid conditions, accurately quantifying crop evapotranspiration is crucial for effective irrigation scheduling. This helps in managing crop water stress and optimizing water productivity. A stress coefficient is commonly employed to evaluate the impact of soil water shortage on crop evapotranspiration. Estimating actual evapotranspiration (ETa) is pivotal in achieving desired crop water use targets and maintaining soil water levels that prevent stress and support satisfactory yields.

While certain plant-based indicators like leaf water potential, stomatal resistance, or canopy temperature can be used to monitor the existing levels of plant stress, approximating ETa remains essential. This approximation allows irrigation regulation to stay within optimal ranges that minimize water consumption without subjecting the plants to excessive stress and subsequent yield losses. The Crop Water Stress Index (CWSI) is a tool to assess the reduction in ETa resulting from water stress.

The CWSI is estimated as the ratio between the actual and potential evapotranspiration. The actual ET was calculated using the SEBS model, which means it is under the normal condition of the field, while the potential ET was estimated using the Penman-Monteith equation multiplied by the crop coefficient with the assumption that the plant is under standard conditions where there is no water stress. The value of the CWSI ranges from 0 to 1, where 0 means that there is no stress and 1 means that the stress reaches the highest value. The growing season has been divided into three phases: initial and development stage, mid-season, and late season, as shown in Figures 8, 9, and 10.

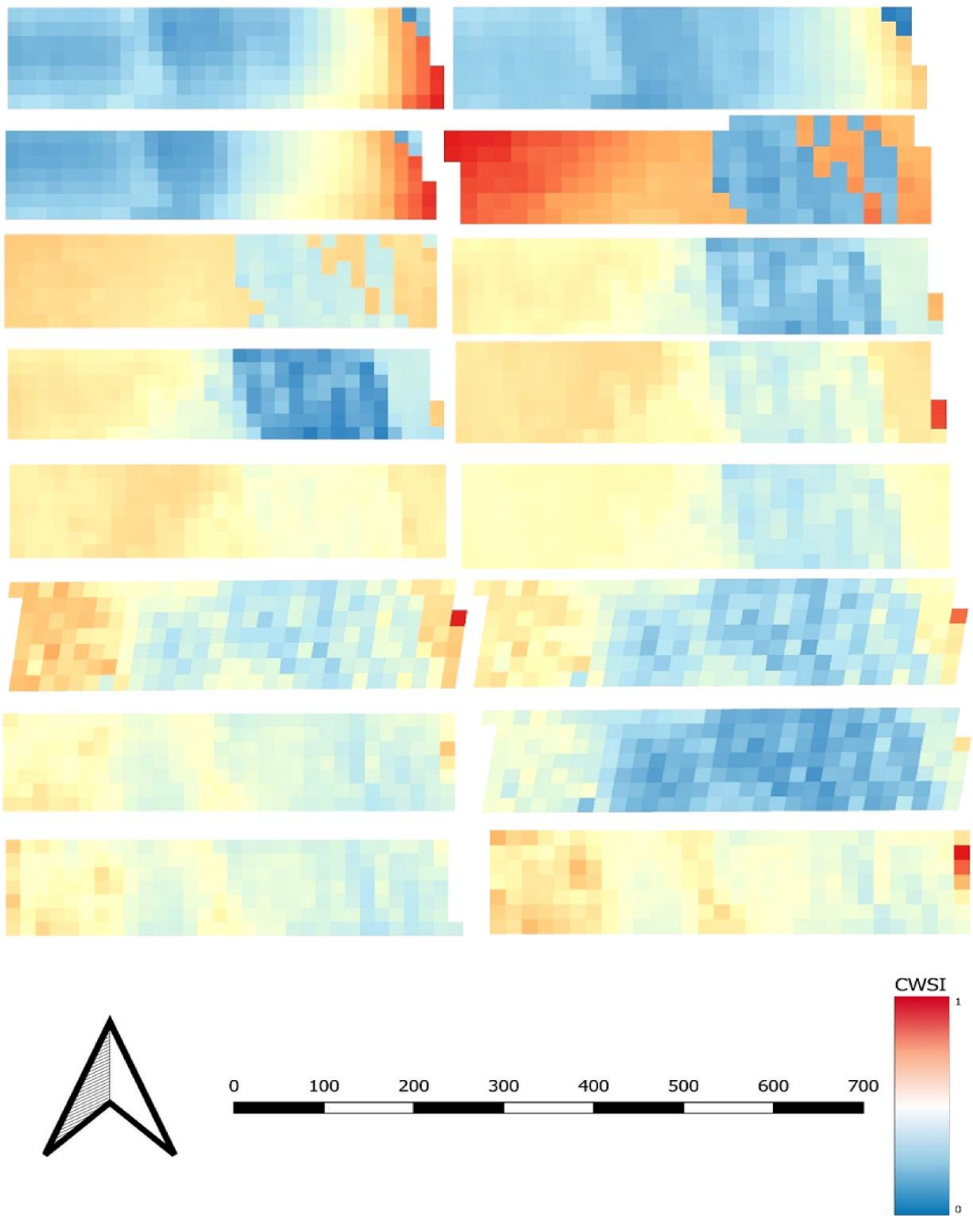

Figure 4. Crop water stress maps for the available dates December 2017 site (A).

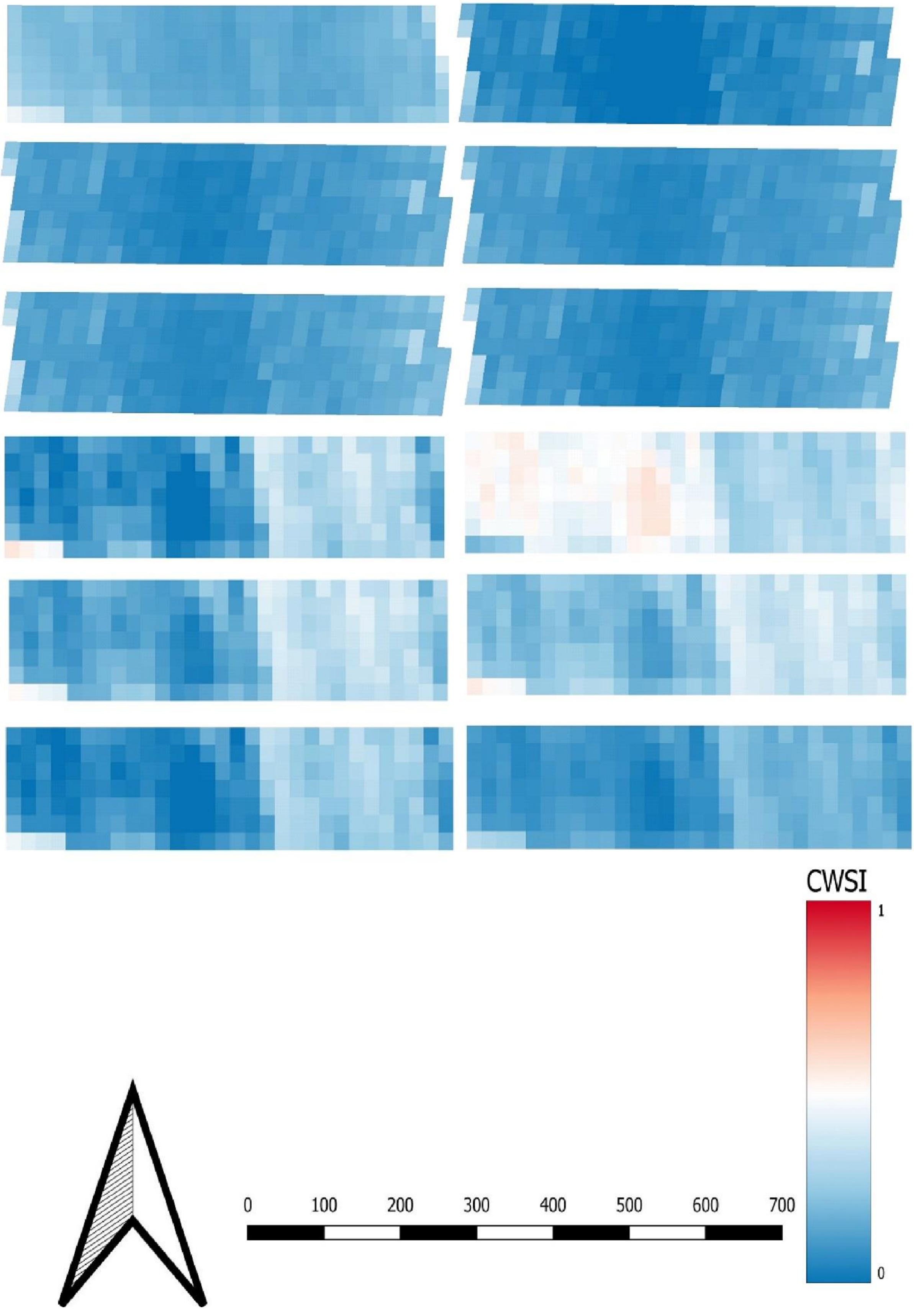

Figure 9. Crop water stress maps for the available dates February 2018 site (A).

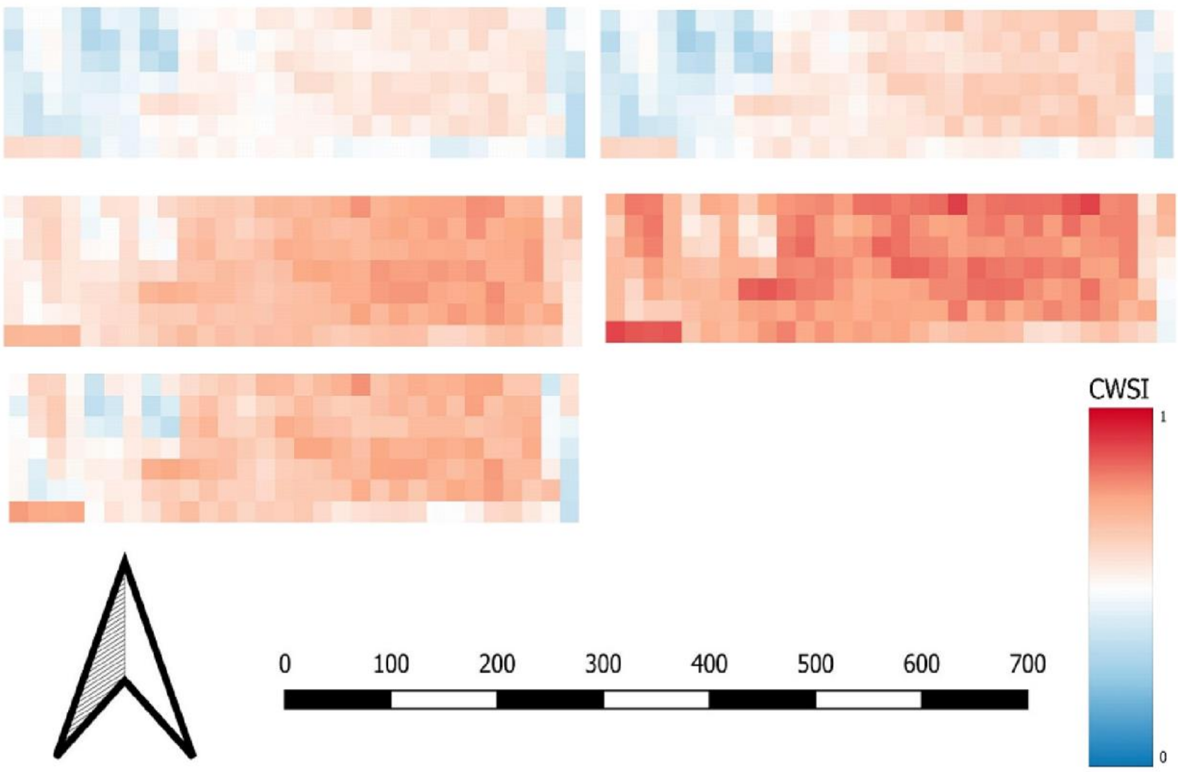

Figure 10. Crop water stress maps for the available dates March 2018 site (A).

Based on the results of monitoring crop water stress, we can indicate that CWS maps can provide valuable information about the health and productivity of crops. The results show that crop water stress maps can estimate the difference between fields; this suggests that the maps can be a useful tool for farmers and agronomists to manage their crops more effectively.

By identifying areas of high and low water stress, farmers can adjust irrigation schedules or other management practices to optimize crop growth and yield. They can irrigate more frequently in areas with high water stress and reduce irrigation in areas with low water stress to avoid overwatering and wasting resources.

In conclusion, the ability to estimate differences in crop water stress between fields through maps is a valuable tool for improving crop management and productivity. By monitoring water stress, farmers and agronomists can make informed decisions regarding irrigation and other management practices, leading to more efficient resource utilization and improved crop yields.

5. CONCLUSIONS AND RECOMMENDATIONS

In this research, a remote sensing-based method was developed to support improving irrigation efficiency under in situ data scarcity conditions. To reach this goal, the following steps were developed:

1. For creating a time series of land surface temperature data with high spatial (30 m) and high temporal (1 day) resolution, the LST downscaling process DisTrad was re-parameterised. The study area has a variety of land cover types. These types include dense vegetation, medium vegetation, low vegetation, bare soil, urban areas, and water. They are in a strongly mosaicked pattern. All the fields are off a small area; therefore, it is difficult to find areas corresponding to the original LST pixels of 1 km resolution with a homogeneous land cover. This loads the definition of the regression parameters between the NDVI and the LST with relatively high uncertainty. To decrease the number of course-resolution pixels with a strongly mixed land cover pattern, we suggested using a smaller number of pixels for the downscaling process in DisTrad. We also recommended to use of linear regression instead of a second-order polynomial since the linear regression is more robust at the edges of the value range. This method helps avoid the extreme values resulting from the second-order polynomial. The results proved that the proposed parameterisation improves the downscaling process in regions with complex land cover, similar to the study area. The coefficient of determination of the linear regression for the downscaled LST was $R^2 = 0.74$ using 25% of the pixels and $R^2 = 0.72$ and using 10% of the pixels in comparison to the $R^2 = 0.61$ of the polynomial regression. This demonstrates that the use of the modified parameters of the DisTrad method resulted in an improvement of the downscaling.
2. The downscaled land surface temperature (LST) with reductions of 10% and 25%, characterized by the lowest coefficient of variation (CV), was employed within the Surface Energy Balance System to estimate actual evapotranspiration at a high spatial resolution. Utilizing downscaled LST resulted in root mean square errors (RMSE) of 0.3 mm day-1 and 0.28 mm day-1 for the downscaling with 10% and 25% reductions in coarse resolution pixels, respectively. In comparison with previous studies ((Bindhu et al., 2013) and (Tan, Wu, & Yan, 2019)), it is evident that our methodology has significantly improved both the temporal and spatial resolution of evapotranspiration estimation. Notably, the coefficient of determination for both downscaling methods (10% and 25%) was nearly identical, registering at 84.5 and 84.1, respectively.

3. The next step was to create a daily ET_a map time series by combining data from different optical sensors. We can conclude that combining data from Landsat 8 and Sentinel 2 is possible due to the strong correlation. This way, a consistent daily ET_a map time series can be created with high spatial and temporal resolution. Even if distortion occurs in the images of one of the sensors, the data of the other sensor can be used as an alternative data source.
4. The crop water productivity in the New Halfa scheme was very low (0.69 $kg.m^{-3}$) compared to the average world crop water productivity of 1.7 $kg.m^{-3}$. This needs to be improved. The efficiency of the irrigation system performance was very low, 60%, compared to the average world irrigation efficiency of the surface irrigation systems (75%).
5. The last step was to evaluate the wheat crop water status using the crop water stress index. Based on the results, we can conclude that the spatial distribution map of the crop water stress helps to plan the spatial and temporal distribution of irrigation, contributing to improved water management.

Finally, we may extrapolate from the indicated findings that these changes enhanced and provided dependable ET_a maps for irrigation scheduling and agricultural planning.

The final recommendation is that earth observation is an optimal method for analysing irrigation performance under data scarcity if the information about the water distribution is available, where it provides information about the water status in the field, which is considered a key point in water management.

In conclusion, this thesis has sought to address critical questions within the scope of its defined parameters. However, it is imperative to acknowledge that our findings represent a snapshot of the ongoing pursuit of knowledge in this field. The complexity and multifaceted nature of the subject matter demand a sustained and rigorous commitment to further investigation. To this end, I recommend that future research endeavours focus on expanding the scope, employing larger sample sizes, employing more varied methodologies, and considering longitudinal approaches where applicable. Moreover, subsequent studies need to explore the nuanced intricacies that this thesis may have left unexamined due to its limitations, such as incorporating the management practices specific to the crops being cultivated.

6. NEW SCIENTIFIC RESULTS

1. I have improved the downscaling of coarse spatial resolution LST by modifying the DisTrad method to make it more robust and reliable for areas with complex land cover. The modifications include the application of linear regression combined with the reduction of the number of sampled pixels.
2. I created a high spatial and temporal resolution daily actual evapotranspiration time series of the New Halfa irrigation scheme from the data of a single satellite to cover the cropping season.
3. I demonstrated that the integration of data from different optical sensors for calculating actual evapotranspiration can result in a homogeneous dataset, which helps to fill gaps in the time series, most frequently caused by cloud cover.
4. Based on the potential and the actual evapotranspiration data I defined the spatial and temporal distribution of water stress and calculated water efficiency in the New Halfa scheme for the 2017/2018 season.
5. I proposed a new approach for optimizing the irrigation schedule in New halfa region by using the crop water stress as indicator for the water status in the field under condition of in situ data scarcity.

References

Agam, N., Kustas, W. P., Anderson, M. C., Li, F., & Neale, C. M. U. (2007). A vegetation index based technique for spatial sharpening of thermal imagery. *Remote Sensing of Environment*, *107*(4), 545–558. https://doi.org/10.1016/j.rse.2006.10.006

Akdim, N., Alfieri, S. M., Habib, A., Choukri, A., Cheruiyot, E., Labbassi, K., & Menenti, M. (2014). *Monitoring of irrigation schemes by remote sensing: Phenology versus retrieval of biophysical variables*. *Remote Sensing* (Vol. 6). https://doi.org/10.3390/rs6065815

Allen, R. G., Pereira, L. S., Raes, D., Smith, M., & Ab, W. (1998). Fao,1998. *Irrigation and Drainage Paper No. 56, FAO*, 300. https://doi.org/10.1016/j.eja.2010.12.001

Allen, R. G., Tasumi, M., & Trezza, R. (2007). Satellite-Based Energy Balance for Mapping Evapotranspiration with Internalized Calibration „ METRIC … — Model, (August), 380–394.

Bastiaanssen, W. G. M., Brito, R. A. L., Bos, M. G., Souza, R. A., Cavalcanti, E. B., & Bakker, M. M. (2001). Low cost satellite data for monthly irrigation performance monitoring: Benchmarks from Nilo Coelho, Brazil. *Irrigation and Drainage Systems*, *15*(1), 53–79. https://doi.org/10.1023/A:1017967021198

Bastiaanssen W.G.M., M. Meneti, R.A. Feddes, Holtslag, a. a M., Bastiaanssen, W. G. M., Menenti, M., … Holtslag, a. a M. (1998). A remote sensing surface energy balance algorithm for land (SEBAL): 1. Formulation. *Journal of Hydrology*, *212–213*(1–4), 198–212. https://doi.org/10.1016/S0022-1694(98)00253-4

Bindhu, V. M., Narasimhan, B., & Sudheer, K. P. (2013). Development and verification of a non-linear disaggregation method (NL-DisTrad) to downscale MODIS land surface temperature to the spatial scale of Landsat thermal data to estimate evapotranspiration. *Remote Sensing of Environment*, *135*, 118–129. https://doi.org/10.1016/j.rse.2013.03.023

Bos, M. G., & Nugteren, J. (1990). On irrigation efficiencies. 4th edition. Wageningen: International Institute for Land Reclamation and Improvement.

Calera, A., Campos, I., Osann, A., D'Urso, G., & Menenti, M. (2017). Remote sensing for crop water management: From ET modelling to services for the end users. *Sensors (Switzerland)*, *17*(5), 1–25. https://doi.org/10.3390/s17051104

Darshana, Pandey, A., Ostrowski, M., & Pandey, R. P. (2012). Simulation and optimization for irrigation and crop planning. *Irrigation and Drainage*, *61*(2), 178–188. https://doi.org/10.1002/ird.633

K. Raju, D. K. (1999). Multicriterion decision making in irrigation planning K.S. *Agricultural Systems*, *62*(1999), 117–129. https://doi.org/10.1002/ird.197

Kustas, W. P., Norman, J. M., Anderson, M. C., & French, A. N. (2003). Estimating subpixel surface temperatures and energy fluxes from the vegetation index-radiometric temperature relationship. *Remote Sensing of Environment*, *85*(4), 429–440. https://doi.org/10.1016/S0034-4257(03)00036-1

Laxén, J. (2007). "Is prosopis a Curse or a Blessing?An ecological-economic analysis of an invasive alien tree species in Sudan ." *Researchgate.Net*. Retrieved from http://www.researchgate.net/publication/237580507_Climate_change_and_African_drylands/file/3deec5202932943c4a.pdf

Molden, D. (1997). Accounting for water use and productivity-SWIM Paper 1.

Roerink, G. J., Su, Z., & Menenti, M. (2000). S-SEBI: A simple remote sensing algorithm to estimate the surface energy balance. *Physics and Chemistry of the Earth, Part B: Hydrology, Oceans and Atmosphere*, *25*(2), 147–157. https://doi.org/10.1016/S1464-1909(99)00128-8

Senay, G. B., Bohms, S., Singh, R. K., Gowda, P. H., Velpuri, N. M., Alemu, H., & Verdin, J. P. (2013). OPERATIONAL EVAPOTRANSPIRATION MAPPING USING REMOTE SENSING AND WEATHER DATASETS : A NEW PARAMETERIZATION FOR THE SSEB APPROACH 1. *JOURNAL OF THE AMERICAN WATER RESOURCES ASSOCIATION*, *49*(3). https://doi.org/10.1111/jawr.12057

Su, Z. (2002). The Surface Energy Balance System (SEBS) for estimation of turbulent heat fluxes. *Hydrology and Earth System Sciences*, *6*(1), 85–100. https://doi.org/10.5194/hess-6-85-2002

Tan, S., Wu, B., & Yan, N. (2019). A method for downscaling daily evapotranspiration based on 30-m surface resistance. *Journal of Hydrology*, *577*(July), 123882. https://doi.org/10.1016/j.jhydrol.2019.06.054

Wallin, M. (2014). *Resettled for Development – The Case of New Halfa Agricultural Scheme, Sudan*. *Current African Issues* (Vol. 59).

Wang, H., Zhang, L., Dawes, W. R., & Liu, C. (2001). Improving water use efficiency of irrigated crops in the North China Plain - Measurements and modelling. *Agricultural Water Management*. https://doi.org/10.1016/S0378-3774(00)00118-9